

Charge retention by peptide ions soft-landed onto self-assembled monolayer surfaces

Julia Laskin^{a,*}, Peng Wang^a, Omar Hadjar^a,
Jean H. Futrell^a, Jormarie Alvarez^b, R. Graham Cooks^b

^a Pacific Northwest National Laboratory, Fundamental Science Directorate, Richland, WA 99352, USA

^b Purdue University, Department of Chemistry, West Lafayette, IN 47907, USA

Received 28 November 2006; received in revised form 9 February 2007; accepted 10 February 2007

Available online 15 February 2007

Abstract

Soft-landing of singly and doubly protonated peptide ions onto three self-assembled monolayer surfaces (SAMs) was performed using a novel ion deposition instrument constructed in our laboratory and a Fourier transform ion cyclotron resonance mass spectrometer (FT-ICR MS) specially designed for studying collisions of large ions with surfaces. Modified surfaces were analyzed using *in situ* 2 keV Cs⁺ secondary ion mass spectrometry or *ex situ* 15 keV Ga⁺ time-of-flight-secondary ion mass spectrometry (ToF-SIMS). The results demonstrate that a fraction of multiply protonated peptide ions retain more than one proton following soft-landing on the FSAM surface. It is shown that the [M+2H]²⁺ ions observed in FT-ICR SIMS spectra are produced by desorption of multiply charged ions from the surface, while re-ionization of singly protonated ions or neutral peptides is a source of [M+2H]²⁺ ions in ToF-SIMS spectra. Differences in neutralization efficiency of soft-landed ions following exposure of surfaces to laboratory air has a measurable effect on the results of *ex situ* ToF-SIMS analysis of soft-landed ions on SAM surfaces. © 2007 Elsevier B.V. All rights reserved.

Keywords: Surface-induced dissociation; Ion soft-landing; Ion-surface collisions; Peptides; Self-assembled monolayers; Secondary ion mass spectrometry (SIMS); Fourier transform ion cyclotron resonance mass spectrometry (FT-ICR MS)

1. Introduction

Soft-landing (SL) of ions on surfaces is a dominant process during interaction of low-energy (<100 eV) ions with semi-conductive targets [1–3]. SL is defined as the intact capture in the condensed phase (surfaces of solids or liquids) of mass-selected polyatomic ions. Physical properties of the surface play a crucial role in determining the outcome of ion-surface collisions [1,4,5]. For example, collisions of ions with clean metal targets result in neutralization of more than 99% of projectile ions, while organic thin films on metal substrates substantially reduce neutralization and increase the fraction of scattered ions [4,6]. Inert semi-conductive surfaces also facilitate charge retention by soft-landed ions [1–3]. Charge retention has been unambigu-

ously proven for small closed-shell ions [7,8] and peptide ions [9] deposited onto fluorinated self-assembled monolayer surfaces (FSAM). SL of proteins with retention of structure has been observed at FSAM surfaces, while retention of configuration and biological activity (but not charge) has been observed for protein landing at liquid surfaces [10,11] and at plasma treated metal surfaces [12]. It has been proposed that SL can be utilized for specific modifications of surfaces (including SAM surfaces) using a beam of mass selected ions of selected size and composition.

We recently conducted a systematic study of several factors that affect SL of peptide ions on inert SAM surfaces [9]. In that work *in situ* analysis of surfaces following SL was performed using 2 keV Cs⁺ secondary ion mass spectrometry (SIMS). We presented evidence that some or all peptide ions retain at least one proton after SL on FSAM surfaces. We further demonstrated that peptide fragments observed in SIMS spectra at all collision energies were produced in the analysis step rather than during ion soft-landing and concluded that intact peptide ions are deposited on FSAM surfaces even at high kinetic energies (at least up to 150 eV). This finding contrasts with previous SID studies that

* Corresponding author at: Fundamental Sciences Division, Pacific Northwest National Laboratory, P.O. Box 999 K8-88, Richland, WA 99352, USA.
Tel.: +1 509 376 4443; fax: +1 509 376 6066.

E-mail address: Julia.Laskin@pnl.gov (J. Laskin).

demonstrated efficient fragmentation of peptide ions scattered off FSAM surfaces at collision energies between 20 and 60 eV [4,5,13–15]. One may infer that the average internal energy of scattered ions is substantially higher than the average internal energy of ions retained on the surface. A plausible rationale of our observations is that scattered ions recoil from the surface in a single repulsive collision while ions that undergo multiple collisions remain trapped on the surface and are thermalized before they can dissociate [9]. Deposition of intact peptide ions has been also demonstrated by Turecek and co-workers for plasma treated metal surfaces as SL targets [16].

In the present research, we further explore charge retention and neutralization (through proton transfer) of peptide ions soft-landed on SAM surfaces by examining fragmentation patterns obtained in SIMS spectra. Specifically, we will compare SIMS spectra of singly, doubly and triply protonated peptides deposited on three different SAM surfaces: inert hydrophobic SAMs of alkylthiol and fluorinated alkylthiol on gold and reactive COOH-terminated SAM. The differences in chemical and physical properties of these surfaces have a profound effect both on the energy transfer in collisions and on the degree of neutralization following SL [1–5].

2. Experimental

2.1. Mass spectrometry

Experiments were performed using a custom built 6T Fourier transform ion cyclotron resonance (FT-ICR) instrument specially configured for studying ion-surface interactions [17] and a novel ion deposition instrument that has been recently constructed in our PNNL laboratory [18]. The FT-ICR instrument and the experimental protocol for SID and SL experiments have been detailed elsewhere [17,18]. Our experimental approach involves normal-incidence collision of externally produced ions with a SAM surface positioned at the rear trapping plate of the ICR cell. Ions are produced in a high-transmission electrospray source, mass-selected and efficiently thermalized in the electrospray interface prior to acceleration and collision with the surface. The ion kinetic energy is controlled by varying the voltage difference between the collisional quadrupole of the ion source and the surface. In this study, the kinetic energy of soft-landed ions was 30 eV. For SL experiments, the surface is exposed to a continuous beam of mass-selected ions. A similar approach is used for SL of mass-selected ions using the ion deposition chamber. *In situ* analysis of surfaces following SL is performed by combining 2 keV Cs⁺ secondary ion mass spectrometry with FT-ICR detection of the sputtered ions (FT-ICR-SIMS) [19]. *Ex situ* analysis of surfaces prepared using the ion deposition instrument was performed using a 15 keV Ga⁺ source time-of-flight-secondary ion mass spectrometer (ToF-SIMS).

In the FTICR SID experiments [18], mass-selected ions are accumulated in a third quadrupole that is held at elevated pressure of about 2×10^{-3} Torr for collisional relaxation of any internal energy possessed by ions generated by electrospray ionization prior to their injection into the ICR cell. After accu-

mulation, the ions are extracted from the third quadrupole and transferred into the ICR cell where they collide with the surface. Ions recoiling from the surface are trapped in the ICR cell and analyzed after a pre-defined reaction delay.

The success of the combination of SIMS and SID with ion trapping in the ICR cell relies on the fact that kinetic energies both of scattered ions formed following normal incidence collisions and of secondary ions generated by surface bombardment with Cs⁺ ions are fairly low (0–10 eV) [15,20]. The unique ICR cell constructed in our laboratory does not perturb the ICR signal as the trapping plate potential is increased from 1 to 50 V [21]. Efficient decoupling the cyclotron, magnetron and axial modes of ion motion in the ICR cell allows us to work with relatively high trapping potentials. This is a great advantage for SID and SIMS studies since it enables us to trap scattered or sputtered ions with a moderate range of kinetic energies quite efficiently, ensuring quantitative detection of ions coming off the surface.

Peptides were purchased from Sigma–Aldrich and Genemed Synthesis, Inc. (South San Francisco, CA) and used as received. Samples were dissolved in a 70:30 or 50:50 (v/v) methanol:water solution with 1% acetic acid to a concentration of 0.1 mg/mL.

2.2. Self-assembled monolayer surfaces

Self-assembled monolayers (SAMs) of 1-dodecanethiol (HSAM), CF₃(CF₂)₉SH (FSAM) and 10-carboxy-1-decanethiol (COOH-SAM) on gold were used as targets. SAMs were prepared following literature procedures [22–24]. The substrates were silicon wafers with a 100 nm gold layer deposited on top of a 10 nm chromium adhesion layer (Structure Probe, Inc., West Chester, PA). After thorough cleaning, the substrates were immersed in 1 mM solutions of the corresponding thiols in ethanol for 12 h. The surfaces were then removed from the solutions, ultrasonically washed in ethanol (10%, v/v, acetic acid in ethanol was used for the COOH-SAM [24]) for 5 min and dried under nitrogen.

3. Results and discussion

Our previous study showed that in a broad range of collision energies from 0 to 150 eV SL of peptide ions results in deposition of intact ions on surfaces [9] and demonstrated that fragmentation observed in the analytical SIMS spectra occurs in the analysis step rather than during ion deposition. Because dissociation of gas-phase peptides and proteins is a strong function of their charge state, [25–27] SIMS fragmentation patterns of soft-landed peptides could provide additional information on charge retention following SL. In this study, we used SIMS to interrogate SAM surfaces following SL of mass-selected ions and examine fragmentation patterns observed in these spectra.

3.1. Charge retention

Fig. 1 is a comparison of the fragmentation behavior observed in the FT-ICR SIMS spectrum of doubly protonated bradykinin deposited on an FSAM surface (Fig. 1a) [28] and 50 eV SID spectra of singly (Fig. 1b) and doubly protonated bradykinin

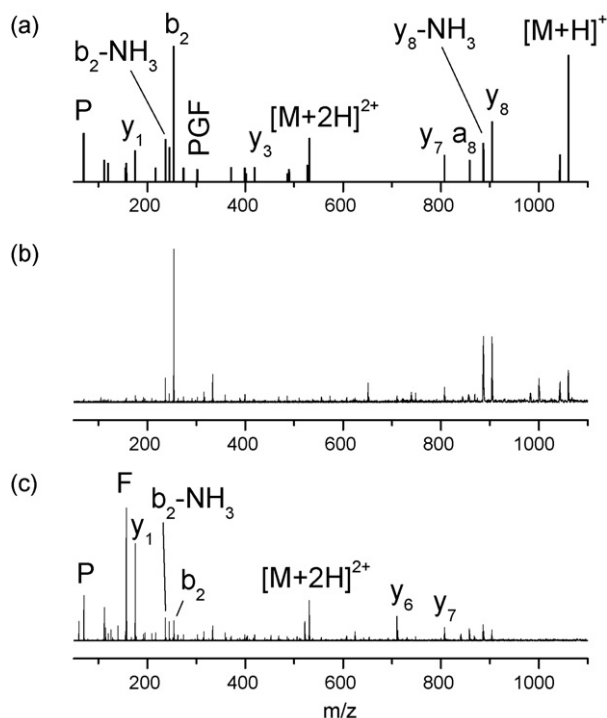


Fig. 1. (a) FT-ICR-SIMS (2 keV Cs⁺) spectrum of doubly protonated bradykinin deposited onto an FSAM surface showing only peptide-related peaks; 50 eV SID spectra of (b) singly and (c) doubly protonated bradykinin on an FSAM surface.

(Fig. 1c). All spectra contain a large number of common peptide backbone fragment ions. Although, the spectra shown in Fig. 1a and b show similarities there are also some obvious differences. For example, low-mass fragments (P, F, y₁) are not observed in the SID spectrum of the [M+H]⁺ ion. In contrast, while the 50 eV SID spectrum of the doubly protonated ion is very different from the SIMS spectrum, it contains abundant low-mass fragments including P, F and y₁ ions. The differences between the two SID spectra are consistent with the well-known tendency of multiply charged peptides to fragment more readily than their singly charged counterparts. We have previously discussed the similarity between SIMS spectra of soft-landed ions and SID spectra of singly protonated peptides [9] and suggested that soft-landed peptides mostly retain one proton regardless of their initial charge state. If only [M+H]⁺ ions were retained on the surface, differences between the SIMS spectrum following SL of the [M+2H]²⁺ ion and the SID spectrum of the [M+H]⁺ ion could be attributed to differences in the internal energy distribution of ions scattered off the surface and ions produced by sputtering. Alternatively, differences between the spectra shown in Fig. 1a and b could be rationalized assuming that a small number of doubly protonated ions are retained on the surface following SL of doubly protonated bradykinin in addition to the dominant singly protonated ions, and these species would contribute features apparent in Fig. 1c to the SIMS spectrum (Fig. 1a).

These two conjectures – which might both contribute – can be distinguished by comparing SID and FT-ICR SIMS obtained following SL of singly protonated precursor ions. Because no doubly protonated ions can be retained on the FSAM sur-

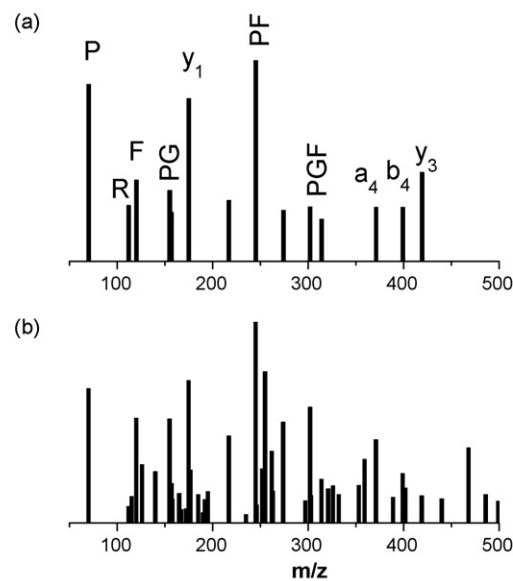


Fig. 2. Low-mass range of the (a) 2 keV Cs⁺ FT-ICR-SIMS spectrum of singly protonated des-Arg¹-bradykinin deposited onto an FSAM surface showing only peptide-related peaks and (b) 50 eV SID spectrum of singly protonated des-Arg¹-bradykinin on an FSAM surface.

face following SL of singly protonated precursors, differences between SID and SIMS spectra necessarily reflect differences in the internal energy distributions deposited into ions by surface collisions and by Cs⁺ bombardment of deposited ions albeit somewhat modified by the effects of ionization of deposited neutrals. Fragmentation patterns obtained for singly protonated des-Arg¹-bradykinin (PPGFSPFR) and angiotensin III (RVY-IHPF) are shown in Figs. 2 and 3. Interestingly, no doubly protonated peptide ion peak was observed in SIMS spectra of soft-landed singly protonated precursors [29] suggesting that

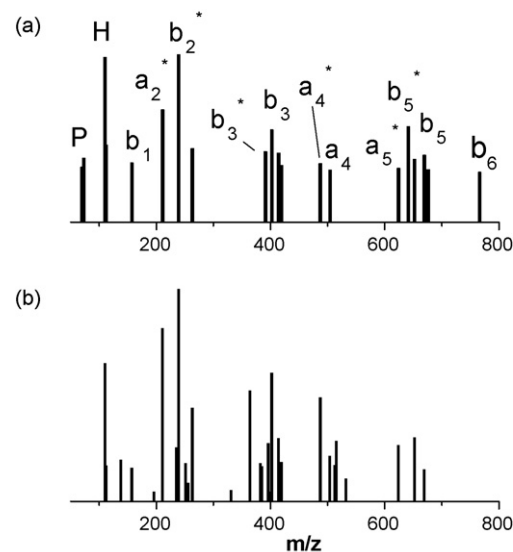


Fig. 3. (a) FT-ICR-SIMS (2 keV Cs⁺) spectrum of singly protonated Angiotensin III deposited onto an FSAM surface showing only peptide-related peaks and (b) 50 eV SID spectrum of singly protonated Angiotensin III on an FSAM surface. An asterisk (*) denotes loss of NH₃ from the corresponding backbone fragment.

$[M+2H]^{2+}$ ions in FT-ICR SIMS spectra are not produced by re-ionization of $[M+H]^+$ ions or neutral peptides. Excellent correspondence between SIMS and 50 eV SID spectra for singly protonated ions suggests that fragments in SIMS spectra shown in Figs. 2 and 3 originate from the singly protonated precursor ions that are either retained on the surface as charged species or re-ionized during Cs^+ bombardment. It is important to note that singly protonated bradykinin is less stable towards dissociation than des-Arg¹-bradykinin and angiotensin III. The collision energy required to observe 50% fragmentation of the precursor ion by collision with the FSAM surface for reaction time of 1 s is 23 eV for singly protonated bradykinin, 28.5 eV for des-Arg¹-bradykinin [30] and 40.5 eV for angiotensin III [31]. In addition, the extent of fragmentation observed for these three systems in FT-ICR SIMS spectra follows the trend in relative stabilities of these ions. Fragmentation efficiencies reported by us previously are 80% for soft-landed bradykinin, 60% for des-Arg¹-bradykinin and 30% for angiotensin III [9]. Our results suggest that while only singly protonated species are retained on the FSAM surface following SL of the corresponding singly protonated precursor ions, retention of both singly and doubly protonated ions occurs in SL of doubly protonated bradykinin. Note that this conclusion is necessary to explain the differences between Fig. 1a and b, as already noted.

Dependence of FT-ICR SIMS spectra on the charge state of the soft-landed ion was further explored by studying 30 eV SL of singly, doubly and triply protonated substance P on the FSAM surface (Fig. 4). These experiments utilized the same ion dose of 6.5×10^{10} ions corresponding to about 5% of a monolayer coverage. Spectra obtained following SL of the singly and doubly protonated substance P (Fig. 4a and b) are quite similar. Although, fragmentation patterns obtained for $[M+H]^+$ and $[M+2H]^{2+}$ precursors are very similar, Fig. 4d demonstrates that fragmentation efficiency is 1.5–2 times higher for the soft-landed doubly protonated precursor ion. In addition, a fairly abundant $[M+2H]^{2+}$ peak and a small peak corresponding to $[M+2H-NH_3]^{2+}$ ion are observed for the doubly protonated precursor but absent from the spectrum obtained for the singly protonated ion. These peaks are very pronounced for triply protonated substance P deposited on the FSAM surface (Fig. 4c). In addition, small b_{10}^{2+} and b_{10} peaks are observed in this spectrum. Both peaks correspond to abundant CID fragments of doubly pro-

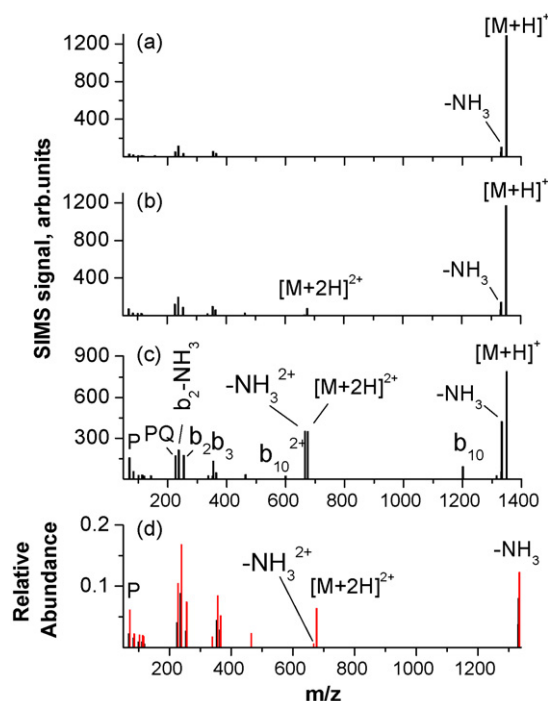


Fig. 4. A 2 keV Cs^+ FT-ICR-SIMS spectra of an FSAM surface following SL of different charge states on Substance P (6.5×10^{10} ions): (a) $[M+H]^+$, (b) $[M+2H]^{2+}$ and (c) $[M+3H]^{3+}$. Panel (d) shows a comparison of spectra shown in panels (a) and (b). All spectra are normalized to the abundance of the $[M+H]^+$ ion.

tonated substance P, while b_{10}^{2+} is also a major CID fragment of the triply protonated precursor [26]. Finally, we note that for the triply protonated precursor ion low-mass fragments are three to four times more abundant than for the singly protonated precursor ion.

In our earlier work, we remarked that very few multiply protonated ions were observed in SIMS spectra [9]. However, careful examination of a large number of FT-ICR SIMS experiments in the present study demonstrated that doubly protonated peptide ions and their respective fragments are not uncommon in FT-ICR SIMS spectra. Relative yields of doubly protonated ions for several precursors are summarized in Table 1. Because FT-ICR signals are proportional to the charge state of the ion [32], abundances of $[M+2H]^{2+}$ ions were divided by a factor of 2

Table 1
Relative yield of doubly protonated ions in SIMS spectra

Peptide	MW	Charge states	$[M+2H]^{2+}/[M+H]^+ \times 100\%$			
			FT-ICR SIMS FSAM	ToF-SIMS		
				FSAM	HSAM	COOH-SAM
Bradykinin (RPPGFSPFR)	1060.5	2	9 ± 5		0.44	4.1 ± 0.8
Gramicidin S (LFPVOLFPVO)	1141.6	1	0	0.3	0.03	0.9 ± 0.8
		2	15 ± 8	0.2	0.05 ± 0.02	1.2 ± 0.7
Substance P (RPKPQQFFGLM-NH ₂)	1347.7	1	0	0.7	0.05	0.12
		2	6 ± 5	2.0	0.04 ± 0.02	1.0 ± 0.8
		3	20 ± 3		0.18	

Error bars were estimated where possible.

in constructing this table. The $[M+2H]^{2+}/[M+H]^+$ ratio shows a strong surface-to-surface variation and in some experiments $[M+2H]^{2+}$ ion is not observed because of insufficient dynamic range of the FT-ICR. Both factors contribute to large error bars listed in Table 1.

Despite the large uncertainties in $[M+2H]^{2+}/[M+H]^+$ ratios, it is clear that the relative abundance of the doubly charged ion observed using *in situ* 2 keV Cs^+ SIMS increases with increase in the charge state of the soft-landed ion. This finding strongly supports the conclusion that peptide ions retain their charge upon SL onto FSAM surfaces. If soft-landed ions were completely neutralized and re-ionized during 2 keV Cs^+ bombardment the $[M+2H]^{2+}/[M+H]^+$ ratio would be independent of the initial charge state of the precursor ion. The increase in the $[M+2H]^{2+}/[M+H]^+$ ratio with increase of the charge state of the soft-landed ion further suggests that a significant fraction of ions retain more than one proton on the FSAM surface.

3.2. *In situ* versus *ex situ* analysis of surfaces

It is interesting to compare these results with results of *ex situ* characterization of surfaces using ToF-SIMS. In these experiments, surfaces are exposed to laboratory air for 15–20 min prior to SIMS analysis. The $[M+2H]^{2+}/[M+H]^+$ ratios obtained using 15 keV Ga^+ ToF-SIMS for three different SAM surfaces are also summarized in Table 1. In general, substantially lower relative abundance of the $[M+2H]^{2+}$ ion is observed using *ex situ* analysis of surfaces following SL. Secondly, the $[M+2H]^{2+}/[M+H]^+$ ratio in ToF-SIMS spectra is largely independent of the initial charge state of the ion. These findings suggest that the most likely pathway for the formation of $[M+2H]^{2+}$ ions in ToF-SIMS is through re-ionization of $[M+H]^+$ ions or neutral peptides on SAM surfaces.

We have previously studied the decay of the SIMS signal as a function of time for surfaces exposed to laboratory air [9]. We showed that two kinetically distinguishable processes contribute to the loss of ca. 85–90% of the sputtered signal: fast decay with lifetime of 10.5 min and slow decay component with lifetime of 77 min. The fast decay that is of interest for this study was attributed to neutralization of soft-landed ions. Preliminary results from our laboratory demonstrate that a significant fraction of soft-landed ions remain charged on the FSAM surface and smaller but measurable fraction of ions survive exposure of the HSAM surface to laboratory air [33]. In contrast, complete neutralization occurs following SL on the COOH-SAM surface. Results shown in Table 1 suggest that neutralization of peptide ions that retain two protons following SL is much more efficient than neutralization of singly protonated ions. The higher $[M+2H]^{2+}/[M+H]^+$ ratio observed for the COOH-SAM surface can be attributed to more efficient re-ionization of peptides on this acidic surface.

Another notable difference between FT-ICR and ToF-SIMS results is that lower fragmentation efficiencies are observed in ToF-SIMS spectra. It should be noted that our FT-ICR SIMS experiments utilize 2 keV Cs^+ ions while ToF-SIMS analysis of surfaces uses 15 keV Ga^+ ion beam, which could affect the results of our comparison between *in situ* and *ex situ* experi-

ments. Yet another difference between these experiments is the observation time. While ToF-SIMS experiments sample ion population few microseconds after bombardment, the residence time for ions in FT-ICR SIMS experiments is on the order of 1 s. Both larger momentum of Ga^+ primary ions and short observation time suppress fragmentation of sputtered ions in ToF-SIMS [34].

3.3. Comparison of different surfaces

Fig. 5 is a comparison of fragmentation patterns observed in FT-ICR SIMS spectra following 30 eV SL of doubly protonated bradykinin and substance P on the HSAM and FSAM surfaces. Clearly, very similar fragmentation patterns are obtained for both peptides on the two surfaces. However, the extent of fragmentation is somewhat higher for the FSAM surface. The observed fragmentation yield for bradykinin is 80% for the HSAM surface and 85% for the FSAM surface. Fragmentation efficiency for substance P is 47% for the HSAM surface and 58% for the FSAM surface. In addition, the relative abundance of the $[M+2H]^{2+}$ ion is two times higher for the FSAM surface. From our earlier discussion, it follows that the somewhat higher fragmentation efficiency observed for the FSAM surface could be attributed to more efficient retention of doubly charged ions on this surface. We have previously demonstrated that SL results in deposition of intact peptide ions on the FSAM surface. Because of the substantial differences in the T → V transfer efficiency in collisions of peptide ions with the FSAM and HSAM surfaces (ca. 20% for the FSAM and 10% for the HSAM surface [4,5]) it is reasonable to assume that SL on the HSAM surface is comparable to FSAM surfaces as a substrate for efficient deposition of intact peptide ions.

It is interesting to note that more abundant a_5 and a_8 fragments of bradykinin are observed on the FSAM surface relative to the HSAM surface. It has been suggested that formation of these fragments involves electronic excitation of the $[M+H]^+$ ion [9,35]. We infer that the extent of electronic excitation in SIMS is higher for the FSAM surface as compared to the HSAM surface.

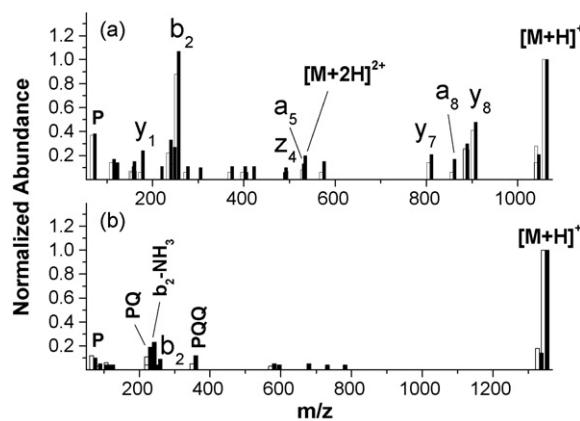


Fig. 5. A 2 keV Cs^+ FT-ICR-SIMS spectra of doubly protonated $[M+2H]^{2+}$ ions of (a) bradykinin and (b) substance P deposited onto FSAM (black bars) and HSAM (white bars) surfaces. All the peaks shown are fragment ions of the peptides. The peaks characteristic of the surface are omitted for simplicity.

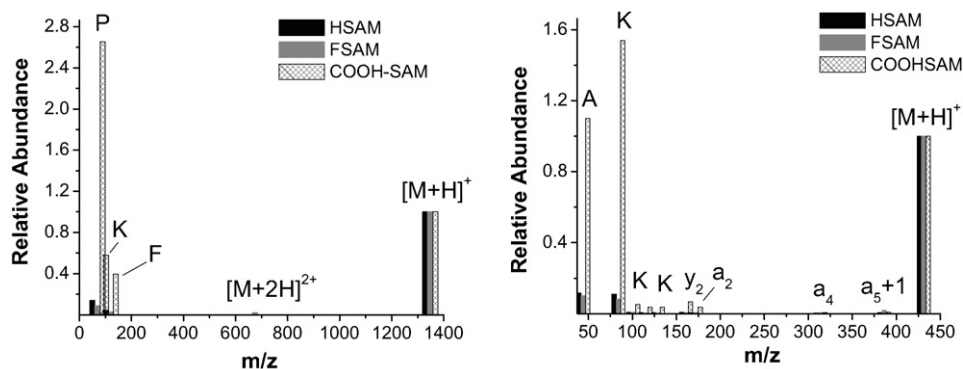


Fig. 6. Abundance of peptide-related peaks normalized to the $[M+H]^+$ ion signal in 15 keV Ga^+ ToF-SIMS spectra of three different surfaces following SL of the (a) doubly protonated Substance P and (b) singly protonated KAAAA peptide.

Fig. 6 shows normalized abundances of peptide fragments observed in ToF-SIMS spectra of three SAM surfaces (HSAM, FSAM and COOH-SAM) following SL of doubly protonated substance P and singly protonated KAAAA pentapeptide. Table 2 summarizes fragmentation efficiencies observed in ToF-SIMS spectra for three different surfaces. The most abundant fragments observed for substance P are immonium ions (P, m/z 70, K, m/z 84, F, m/z 120). Fragmentation of KAAAA is dominated by the formation of immonium ions of lysine (K, m/z 84, 101 and 129) and alanine (A, m/z 44). Other fragments include y_2 (m/z 161), a_2 (m/z 172), a_4 (m/z 314) and $a_5 + 1$ (m/z 386) ions. Strong $[M+H]^+$ peaks were observed in all spectra. The extent of fragmentation in ToF-SIMS spectra of soft-landed ions shows a strong dependence on the type of the SAM surface (see Table 2).

In contrast with the results of *in situ* experiments discussed earlier, more efficient fragmentation is observed in ToF-SIMS spectra of the HSAM surface as compared to the FSAM surface. Exposure of surfaces to laboratory air prior to ToF-SIMS analysis results in partial neutralization of soft-landed ions. Although desorption and ionization of neutral peptide molecules is much less efficient than desorption of ions that retained their charge on the surface, there is a substantial reionized neutral contribution of the peptide signal in ToF-SIMS spectra. Because more efficient neutralization occurs on the HSAM surface as compared to the FSAM surface the contribution from re-ionization of neutral molecules is larger for the HSAM surface. Molecular dynamics simulations show that rather narrow internal energy distributions are deposited into desorbed molecules by 15 keV Ga^+ bombardment [36]. Only 9% of desorbed benzene (m/z 78) and 5% of polystyrene tetramer (m/z 559) molecules have the internal energy sufficient for dissociation on the microsecond timescale of the ToF-SIMS analysis [37]. While dissociation barriers for these relatively small ions are higher than the energy thresholds for dissociation of peptide ions, unimolecular dissociation of peptide ions can be significantly slower because of the

large number of vibrational degrees of freedom. For example, dissociation rate of 10^5 s^{-1} corresponds to the excess internal energy of ca. 5 eV for benzene cation [38] and more than 10 eV for most peptide ions studied by us so far [39]. It follows that molecular dynamics simulations reported for smaller molecules provide the upper limit for the expected fragmentation yield for peptide ions induced by surface bombardment. However, these simulations do not take into account the internal excitation associated with the ionization step. It should be noted that a significant amount of internal energy can be deposited into desorbed molecules during the ionization step because formation of $[M+H]^+$ ions from neutral molecules either by direct proton addition or by proton transfer reactions is an exothermic process. It follows that the counter-intuitive result of the higher fragmentation efficiency found for the HSAM surface could be attributed to a more significant contribution of neutral molecules to the SIMS signal.

This conclusion is further supported by the results obtained using COOH-SAM surface as a soft-landing target. Because of complete neutralization of soft-landed ions on this surface, re-ionization of neutral peptide molecules is the only path for the formation of secondary ions. This process is accompanied by extensive (>70%) fragmentation of secondary ions on the microsecond scale of ToF-SIMS.

Our results suggest that differences in fragmentation efficiencies observed using FSAM, HSAM and COOH-SAM as soft-landing targets can be attributed to different mechanisms of secondary ion formation on these surfaces. Specifically, desorption of ions that retain their charge on the FSAM surface results in substantially lower internal energy deposition than re-ionization of neutral molecules from the COOH-SAM surface, while secondary ion signal obtained from the HSAM surface includes contributions from both processes.

4. Conclusions

This study utilized secondary ions mass spectrometry to explore charge retention and neutralization of peptides soft-landed on FSAM, HSAM and COOH-SAM surfaces. We used FT-ICR SIMS for *in situ* analysis and ToF-SIMS for *ex situ* analysis of surfaces following SL of peptide ions. We found that SL of multiply protonated peptide ions on the FSAM surface

Table 2
Fragmentation efficiencies observed in ToF-SIMS spectra (%)

Precursor ion	Charge state	FSAM	HSAM	COOH-SAM
Substance P	2	13	17	78
KAAAA	1	19	21	74

results in retention of one and two protons. This is reflected in abundant $[M+2H]^{2+}$ ion observed in FT-ICR SIMS spectra following SL of multiply protonated peptide ions not found for singly protonated ions. The presence of doubly charged ions on the FSAM surface is reflected in higher fragmentation efficiency observed in FT-ICR SIMS spectra. In contrast, differences in fragmentation behavior observed in ToF-SIMS spectra are mainly attributed to the differences in the relative contribution of neutral peptide molecules to the secondary ion signal. Exposure of the FSAM and HSAM surfaces to laboratory air results in partial neutralization of soft-landed ions. Desorption and ionization of neutral molecules results in higher internal excitation of secondary ions than direct desorption of ions from the surface. This leads to high fragmentation efficiency for the COOH-SAM surface, which mainly retains neutral peptides. The larger extent of fragmentation observed on the HSAM surface as compared to the FSAM surface is attributed to more efficient neutralization of ions on the HSAM surface. Finally, formation of abundant a-ions in SIMS spectra when FSAM is a SL target suggests that larger fraction of electronically excited ions is sputtered from FSAM surfaces.

Acknowledgements

The research described in this manuscript was performed at the W.R. Wiley Environmental Molecular Sciences Laboratory, A National Scientific user facility sponsored by the U.S. Department of Energy's Office of Biological and Environmental Research and located at Pacific Northwest National Laboratory (PNNL). PNNL is operated by Battelle for the U.S. Department of Energy. Research at EMSL was supported by the grant from the Chemical Sciences Division, Office of Basic Energy Sciences of the US Department of Energy and the by the PNNL Laboratory Directed Research and Development (LDRD) Program. Research at Purdue University was supported by the National Science Foundation (CHE 0412782). Jormarie Alvarez acknowledges participation in the PNNL Interfacial and Condensed Phase Summer Research Institute.

References

- [1] V. Grill, J. Shen, C. Evans, R.G. Cooks, *Rev. Sci. Instrum.* 72 (2001) 3149.
- [2] B. Gologan, J.R. Green, J. Alvarez, J. Laskin, R.G. Cooks, *Phys. Chem. Chem. Phys.* 7 (2005) 1490.
- [3] B. Gologan, J.M. Wiseman, R.G. Cooks, in: J. Laskin, C. Lifshitz (Eds.), *Principles of Mass Spectrometry Applied to Biomolecules*, John Wiley & Sons, Inc., Hoboken, NJ, 2006.
- [4] A.R. Dongre, A. Somogyi, V.H. Wysocki, *J. Mass Spectrom.* 31 (1996) 339.
- [5] J. Laskin, J.H. Futrell, *J. Chem. Phys.* 119 (2003) 3413.
- [6] R.G. Cooks, T. Ast, T. Pradeep, V. Wysocki, *Acc. Chem. Res.* 27 (1994) 316.
- [7] S.A. Miller, H. Luo, S.J. Pachuta, R.G. Cooks, *Science* 275 (1997) 1447.
- [8] H. Luo, S.A. Miller, R.G. Cooks, S.J. Pachuta, *Int. J. Mass Spectrom.* 174 (1998) 193.
- [9] J. Alvarez, J.H. Futrell, J. Laskin, *J. Phys. Chem. A* 110 (2006) 1678.
- [10] Z. Ouyang, Z. Takats, T.A. Blake, B. Gologan, A.J. Guymon, J.M. Wiseman, J.C. Oliver, V.J. Davisson, R.G. Cooks, *Science* 301 (2003) 1351.
- [11] B. Gologan, Z. Takats, J. Alvarez, J.M. Wiseman, N. Talaty, Z. Ouyang, R.G. Cooks, *J. Am. Soc. Mass Spectrom.* 15 (2004) 1874.
- [12] M. Volny, W.T. Elam, A. Branca, B.D. Ratner, F. Tureček, *Anal. Chem.* 77 (2005) 4890.
- [13] E. Stone, K.J. Gillig, B. Ruotolo, K. Fuhrer, M. Gonin, A. Schultz, D.H. Russell, *Anal. Chem.* 73 (2001) 2233.
- [14] J. Laskin, J.H. Futrell, *J. Am. Soc. Mass Spectrom.* 14 (2003) 1340.
- [15] J. Laskin, J.H. Futrell, *Mass Spectrom. Rev.* 24 (2005) 135.
- [16] M. Volny, W.T. Elam, B.D. Ratner, F. Tureček, *Anal. Chem.* 77 (2005) 4846.
- [17] O. Hadjar et al., in preparation.
- [18] J. Laskin, E.V. Denisov, A. Shukla, S.E. Barlow, J.H. Futrell, *Anal. Chem.* 74 (2002) 3255.
- [19] J. Alvarez, R.G. Cooks, S.E. Barlow, D.J. Gaspar, J.H. Futrell, J. Laskin, *Anal. Chem.* 77 (2005) 3452.
- [20] B. Arezki, A. Delcorte, B.J. Garrison, P. Bertrand, *J. Phys. Chem. B* 110 (2006) 6832.
- [21] S.E. Barlow, M.D. Tinkle, *Rev. Sci. Instrum.* 73 (2002) 4185.
- [22] C.E.D. Chidsey, G.Y. Liu, P. Rowntree, G. Scoles, *J. Chem. Phys.* 91 (1989) 4421.
- [23] D. Barriet, T.R. Lee, *Curr. Opin. Colloid Interface Sci.* 8 (2003) 236.
- [24] H. Wang, S.F. Chen, L.Y. Li, S.Y. Jiang, *Langmuir* 21 (2005) 2633.
- [25] K.M. Downard, K. Biemann, *J. Am. Soc. Mass Spectrom.* 5 (1994) 966.
- [26] X.J. Tang, P. Thibault, R.K. Boyd, *Anal. Chem.* 65 (1993) 2824.
- [27] G.E. Reid, J. Wu, P.A. Chrisman, J.M. Wells, S.A. McLuckey, *Anal. Chem.* 73 (2001) 3274.
- [28] The reviewer noticed that spectrum shown in Fig. 1a shows the $[M+2H]^{2+}$ peak while Fig. 2a from Ref. [9] that was obtained under similar condition does not contain the doubly charged ion of bradykinin. In fact, the $[M+2H]^{2+}$ peak is present in Fig. 2a of Ref. [9] but is not labeled along with many other peaks in the spectrum.
- [29] Because of the limited dynamic range of our FT-ICR SIMS experiments we could not detect ions with relative abundance of <1% of the $[M+H]^+$ peak.
- [30] J. Laskin, T.H. Bailey, E.V. Denisov, J.H. Futrell, *J. Phys. Chem. A* 106 (2002) 9832.
- [31] J. Laskin, T.H. Bailey, J.H. Futrell, *Int. J. Mass Spectrom.* 234 (2004) 89.
- [32] M.B. Comisarow, *J. Chem. Phys.* 69 (1978) 4097.
- [33] P. Wang, J. Laskin, unpublished results.
- [34] R.G. Orth, H.T. Jonkman, J. Michl, *J. Am. Chem. Soc.* 104 (1982) 1834.
- [35] S.B. Nielsen, J.U. Andersen, P. Hvelplund, T.J.D. Jorgensen, M. Sorensen, S. Tomita, *Int. J. Mass Spectrom.* 213 (2002) 225.
- [36] Z. Postawa, B. Czerwinski, N. Winograd, B.J. Garrison, *J. Phys. Chem. B* 109 (2005) 11973.
- [37] B. Czerwinski, A. Delcorte, B. Garrison, R. Samson, N. Winograd, Z. Postawa, *Appl. Surf. Sci.* 252 (2006) 6419.
- [38] T.L. Grebner, H.J. Neusser, *Int. J. Mass Spectrom.* 187 (1999) 517.
- [39] J. Laskin, in: J. Laskin, C. Lifshitz (Eds.), *Principles of Mass Spectrometry Applied to Biomolecules*, John Wiley & Sons, Inc., Hoboken, NJ, 2006.